

## RESEARCH REPORT

# Neuropilin 1 (NRP1) hypomorphism combined with defective VEGF-A binding reveals novel roles for NRP1 in developmental and pathological angiogenesis

Alessandro Fantin<sup>1,\*</sup>, Birger Herzog<sup>2,\*</sup>, Marwa Mahmoud<sup>2,‡</sup>, Maiko Yamaji<sup>2,‡</sup>, Alice Plein<sup>1</sup>, Laura Denti<sup>1</sup>, Christiana Ruhrberg<sup>1,§</sup> and Ian Zachary<sup>2,§</sup>

## ABSTRACT

Neuropilin 1 (NRP1) is a receptor for class 3 semaphorins and vascular endothelial growth factor (VEGF) A and is essential for cardiovascular development. Biochemical evidence supports a model for NRP1 function in which VEGF binding induces complex formation between NRP1 and VEGFR2 to enhance endothelial VEGF signalling. However, the relevance of VEGF binding to NRP1 for angiogenesis *in vivo* has not yet been examined. We therefore generated knock-in mice expressing *Nrp1* with a mutation of tyrosine (Y) 297 in the VEGF binding pocket of the NRP1 b1 domain, as this residue was previously shown to be important for high affinity VEGF binding and NRP1-VEGFR2 complex formation. Unexpectedly, this targeting strategy also severely reduced NRP1 expression and therefore generated a NRP1 hypomorph. Despite the loss of VEGF binding and attenuated NRP1 expression, homozygous *Nrp1*<sup>Y297A/Y297A</sup> mice were born at normal Mendelian ratios, arguing against NRP1 functioning exclusively as a VEGF<sub>165</sub> receptor in embryonic angiogenesis. By overcoming the mid-gestation lethality of full *Nrp1*-null mice, homozygous *Nrp1*<sup>Y297A/Y297A</sup> mice revealed essential roles for NRP1 in postnatal angiogenesis and arteriogenesis in the heart and retina, pathological neovascularisation of the retina and angiogenesis-dependent tumour growth.

**KEY WORDS:** NRP1, VEGF, Angiogenesis, Arteriogenesis, Retina, Hindbrain

## INTRODUCTION

NRP1 is a transmembrane receptor for the VEGF<sub>165</sub> isoform (VEGF<sub>164</sub> in mice) and the neuronal guidance cue SEMA3A, with essential roles in both vascular and neuronal development (reviewed by Pellet-Many et al., 2008; Raimondi and Ruhrberg, 2013). Accordingly, *Nrp1*-null mice die before birth with severe cardiovascular and neuronal defects (Kitsukawa et al., 1997; Kawasaki et al., 1999). Mice lacking NRP1 in vascular endothelial cells (ECs) also show defective cardiovascular development,

whereas mice carrying a mutated extracellular domain that abolishes SEMA3A, not VEGF<sub>164</sub>, binding show defective nerve, but not blood vessel, patterning (Gu et al., 2003; Vieira et al., 2007). These and other genetic, biochemical and cell biological data support a model in which VEGF<sub>165</sub> binding induces complex formation between NRP1 and VEGFR2 (KDR – Mouse Genome Informatics) to enhance VEGFR2 signalling during EC migration *in vitro* (e.g. Soker et al., 2002; Wang et al., 2003; Evans et al., 2011) and arteriogenesis *in vivo* (Lanahan et al., 2013).

The extracellular NRP1 a1/a2 and b1/b2 domains are crucial for recognition of SEMA3A, whereas the major VEGF binding site resides in the b1 domain, with some contribution of the b2 domain (Gu et al., 2002). Structural studies of the b1 domain have identified key residues important for ligand interactions in a VEGF<sub>165</sub>-binding pocket (von Wronski et al., 2006; Vander Kooi et al., 2007; Jarvis et al., 2010). For example, mutation of Y297 or D320 in the b1 domain impairs VEGF<sub>165</sub> binding and complex formation between NRP1 and VEGFR2, which reduces VEGF<sub>165</sub>-stimulated EC migration *in vitro* (Jarvis et al., 2010; Herzog et al., 2011).

Though NRP1 is essential for developmental angiogenesis, the contribution of the NRP1-VEGF interaction to physiological or pathological angiogenesis is unclear. We therefore generated mice with a Y297A mutation in the b1 VEGF binding site (supplementary material Fig. S1A). Inadvertently, insertion of a *Nrp1*<sup>Y297A</sup> mutant cDNA reduced mRNA and protein expression of the mutant allele, generating a novel mouse model with NRP1 hypomorphism. Despite combining loss of VEGF binding with reduced NRP1 expression, *Nrp1*<sup>Y297A/Y297A</sup> homozygous mice were mostly viable at birth, without the severe and lethal cardiovascular phenotypes of full or endothelial-specific *Nrp1*-null mutants. This observation implies that NRP1 has important VEGF-independent roles in angiogenesis which most likely synergise with its known role as a VEGFR2 co-receptor. Moreover, the postnatal viability of *Nrp1*<sup>Y297A/Y297A</sup> mice enabled the study of newborn and adult mutants, thereby extending genetic evidence for the established function of NRP1 in cardiovascular development to include essential roles in promoting postnatal and pathological angiogenesis.

## RESULTS AND DISCUSSION

## Reduced NRP1 expression in *Nrp1*<sup>Y297A/Y297A</sup> mice

Previous studies demonstrated that the highly conserved Y297 residue in the NRP1 b1 domain (supplementary material Fig. S1A,B) is essential for VEGF<sub>165</sub> binding to human NRP1 (Jarvis et al., 2010; Herzog et al., 2011). The Y297A mutation also inhibited high affinity binding of <sup>125</sup>I-VEGF<sub>165</sub> to murine NRP1 *in vitro* (supplementary material Fig. S1C). Heterozygous mice expressing a mutated *Nrp1*<sup>Y297A</sup> cDNA from exon 2 of the

<sup>1</sup>UCL Institute of Ophthalmology, University College London, 11-43 Bath Street, London EC1V 9EL, UK. <sup>2</sup>Centre for Cardiovascular Biology and Medicine, BHF Laboratories, Division of Medicine, University College London, 5 University Street, London WC1E 6JJ, UK.

\*These authors contributed equally to this work

‡These authors contributed equally to this work

§Authors for correspondence (I.Zachary@ucl.ac.uk; c.ruhrberg@ucl.ac.uk)

This is an Open Access article distributed under the terms of the Creative Commons Attribution License (<http://creativecommons.org/licenses/by/3.0>), which permits unrestricted use, distribution and reproduction in any medium provided that the original work is properly attributed.

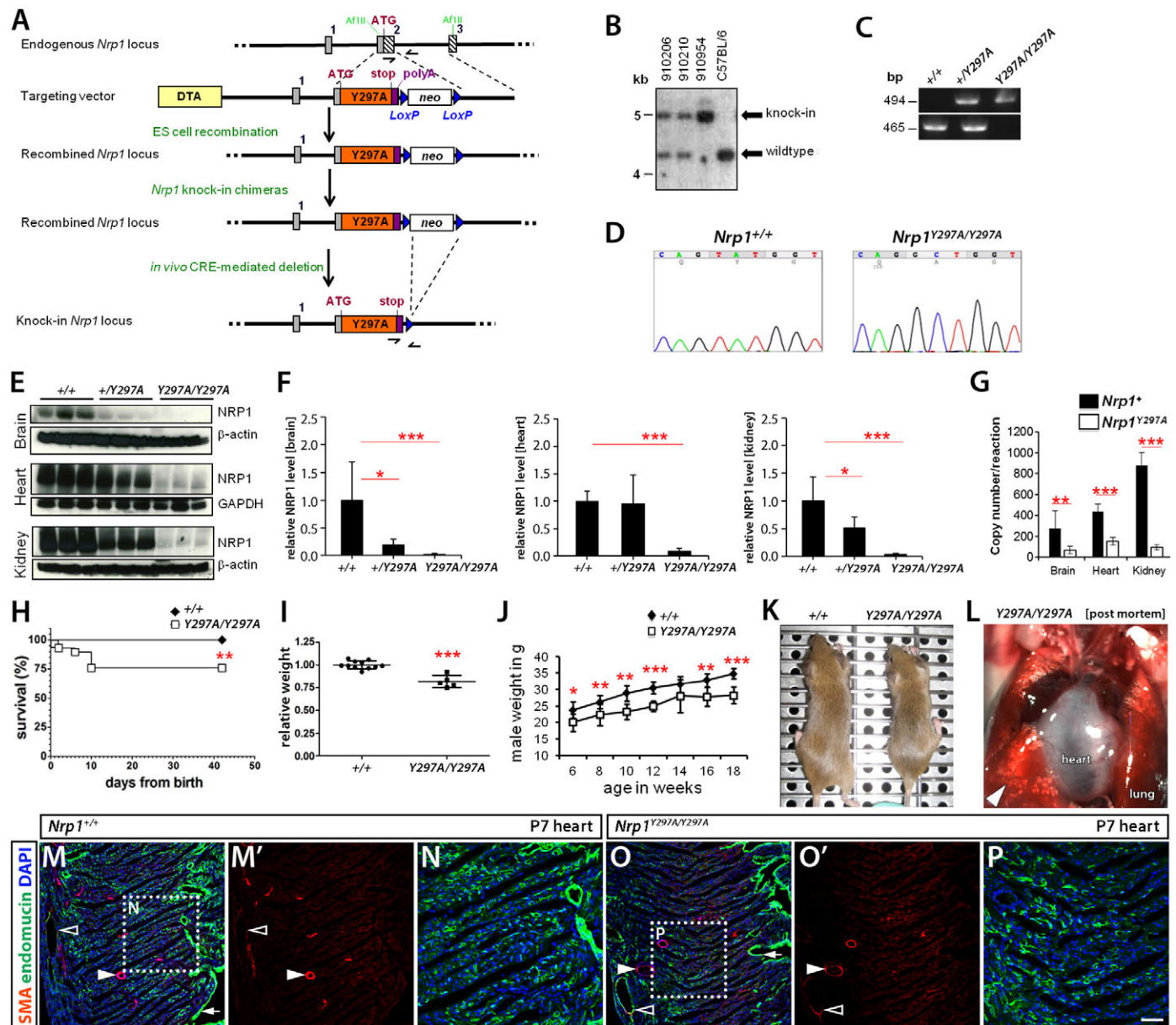


**Fig. 1. *Nrp1*<sup>Y297A/Y297A</sup> mice have reduced NRP1 expression, survival, body weight and heart vascularisation.** (A) Mouse *Nrp1* cDNA with a Y297A substitution was used to target exon 2 of the endogenous *Nrp1* locus. (B) Southern blot of *Afl*III-digested genomic DNA from WT and gene-targeted mice after removal of the neomycin cassette. (C) PCR analysis of WT and mutant alleles. (D) cDNA sequencing of WT and homozygous mice. (E,F) NRP1 levels in immunoblots were quantified by densitometry relative to GAPDH or  $\beta$ -actin (mean  $\pm$  s.d.;  $n=6$  each). (G) *Nrp1* mRNA expression from WT (black bars) and *Nrp1*<sup>Y297A</sup> (white bars) alleles in *Nrp1*<sup>+/Y297A</sup> mice was determined by TaqMan qPCR (mean  $\pm$  s.d.;  $n=6$ ). (H) Survival of WT and *Nrp1*<sup>Y297A/Y297A</sup> littermates during the first 6 weeks of postnatal life ( $n \geq 27$ ). (I) Body weights of WT and *Nrp1*<sup>Y297A/Y297A</sup> littermates at P7 ( $n=5-11$ ; mean  $\pm$  s.d.). (J) Body weight of WT and *Nrp1*<sup>Y297A/Y297A</sup> males between 6 and 18 weeks ( $n=3-10$  animals per group and genotype; mean  $\pm$  s.d.). (K) Appearance of 6-week-old WT and *Nrp1*<sup>Y297A/Y297A</sup> littermates. (L) Post mortem analysis of a suddenly deceased P7 *Nrp1*<sup>Y297A/Y297A</sup> pup. Arrowhead indicates blood-filled lungs. (M-P) Immunostaining for endomucin (green), SMA (red) and DAPI (blue) of P7 heart cryosections from WT and *Nrp1*<sup>Y297A/Y297A</sup> littermates. (M',O') Single SMA channels of panels M,O. (N,P) High magnification image of insets in panels M,O. Arrowheads indicate SMA+ endomucin- coronary arteries; open arrowheads indicate SMA+ endomucin+ coronary vein; arrows indicate endocardium;  $n=3$  each. \* $P < 0.05$ , \*\* $P < 0.01$ , \*\*\* $P < 0.001$  *Nrp1*<sup>Y297A/Y297A</sup> or *Nrp1*<sup>+/Y297A</sup> versus WT. Scale bar: 100  $\mu$ m (M-P).

endogenous *Nrp1* locus were generated (Fig. 1A) and interbred to produce homozygous *Nrp1*<sup>Y297A/Y297A</sup> offspring (Fig. 1B-D). Unexpectedly, immunoblotting revealed a severe reduction of NRP1 in *Nrp1*<sup>Y297A/Y297A</sup> and a moderate reduction in *Nrp1*<sup>Y297A/+</sup> mice compared with wild-type (WT) littermates (Fig. 1E,F). Immunohistochemistry confirmed reduced NRP1 expression in *Nrp1*<sup>Y297A/Y297A</sup> tissues (supplementary material Fig. S2A,B).

Reduced NRP1 protein levels correlated with decreased *Nrp1* mRNA expression in all *Nrp1*<sup>Y297A/Y297A</sup> tissues examined (supplementary material Fig. S2C). Impaired expression of the *Nrp1*<sup>Y297A</sup> allele may be due to the disruption of intronic regulatory elements deleted by insertion of the mutant cDNA into the *Nrp1* locus. Allele-specific quantitative PCR (qPCR) of heterozygous mice demonstrated significantly reduced expression of the mutant

allele compared with the WT allele in all tissues examined (Fig. 1G). Mice expressing the *Nrp1*<sup>Y297A</sup> allele are therefore hypomorphic for NRP1 with markedly reduced NRP1 expression as well as reduced VEGF<sub>164</sub> binding and represent a novel model in which to examine NRP1 roles in angiogenesis *in vivo*.

### Increased mortality and impaired growth in postnatal *Nrp1*<sup>Y297A/Y297A</sup> mice

Genotyping of offspring from crosses between heterozygous mice yielded the expected Mendelian ratio for WT, heterozygous and homozygous mice before birth, and only a small, non-significant reduction in the number of *Nrp1*<sup>Y297A/Y297A</sup> offspring on postnatal day (P) 0 (supplementary material Table S2), indicating that residual NRP1 expression from the *Nrp1*<sup>Y297A</sup> allele prevents the mid-gestation lethality of full NRP1 knockouts. By contrast, homozygous mutants were under-represented in litters at P21, and the number of adult *Nrp1*<sup>Y297A/Y297A</sup> mice (>8 weeks) was ~50% lower than expected (supplementary material Table S2). Follow-up from birth to 6 weeks of age showed increased mortality of *Nrp1*<sup>Y297A/Y297A</sup> mice predominantly within the first 2 weeks of postnatal life (Fig. 1H). *Nrp1*<sup>Y297A/Y297A</sup> mice were also significantly smaller than WT littermates at P7 (Fig. 1I) and at all ages examined between 6 and 18 weeks (Fig. 1J,K). Heterozygous mice had normal weights at P7, but showed a small, significant size reduction at 8, 10, 12 and 14 weeks (data not shown). These results indicate that low NRP1 expression combined with inhibition of VEGF<sub>164</sub> binding causes postnatal mortality and reduces body weight in surviving mice.

### Defective myocardial vascularisation in postnatal *Nrp1*<sup>Y297A/Y297A</sup> mice

Post mortem analysis of mutants that had died on P7 revealed blood-filled lungs (Fig. 1L), indicative of congestive heart failure. Increased mortality and reduced body size are also seen in *Vegfa*<sup>120/120</sup> mutants that die perinatally owing to ischemic cardiomyopathy caused by impaired myocardial vascularisation (Carmeliet et al., 1999). Similarly, P7 *Nrp1*<sup>Y297A/Y297A</sup> hearts contained fewer coronary arteries and capillaries than control hearts (Fig. 1M-P). Moreover, capillaries in mutants appeared abnormal and were sparse, particularly in the subendomyocardium, consistent with reports that angiogenesis occurs in an epicardial-to-endocardial gradient (Tomanek, 1996). The similar vascular defects in *Nrp1*<sup>Y297A/Y297A</sup> and *Vegfa*<sup>120/120</sup> myocardium, combined with a predominance of NRP1-binding VEGF isoforms relative to VEGF<sub>120</sub> in this tissue (Ng et al., 2001), suggest that the perinatal vascularisation of myocardium depends on VEGF binding to NRP1.

### Embryonic angiogenesis is mildly impaired in *Nrp1*<sup>Y297A/Y297A</sup> mutants

We next investigated the effect of the Y297A mutation on VEGF binding to NRP1 and on vascular development in the hindbrain on embryonic days (E) 11.5 and E12.5, when blood vessels sprout and fuse to form the subventricular vascular plexus (SVP) (Fantin et al., 2010). Although *Nrp2*, *Vegfr1* (*Flt1* – Mouse Genome Informatics) and *Vegfr2* mRNA levels were unaffected, *Nrp1* transcripts were reduced by 50% in *Nrp1*<sup>Y297A/Y297A</sup> compared with WT hindbrains (Fig. 2A). In agreement, immunostaining showed reduced NRP1 protein levels in the mutants, both in axons and vessels (Fig. 2B,C). Alkaline phosphatase (AP)-conjugated VEGF<sub>165</sub> ligand binding to NRP1-positive pial axons was abolished in *Nrp1*<sup>Y297A/Y297A</sup> mutant, similar to *Nrp1*-null, hindbrains (Fig. 2D). By contrast, AP-VEGF<sub>165</sub> binding to vessels was unaffected (Fig. 2D), consistent with high VEGFR2

expression by hindbrain ECs, but not axons (Lanahan et al., 2013). AP-SEMA3A binding to NRP1-expressing axons in *Nrp1*<sup>Y297A/Y297A</sup> mice was unperturbed (Fig. 2E). However, AP-SEMA3A binding to SVP vessels was impaired, even though binding to radial vessels on the pial side was unaffected (Fig. 2E), perhaps due to the differential effect of the *Nrp1* mutation on overall NRP1 protein levels in the two brain regions.

E12.5 *Nrp1*<sup>Y297A/Y297A</sup> hindbrains exhibited a similar number of radial vessels compared with WT littermates (Fig. 2F,G), but significantly reduced vessel branching in the SVP (Fig. 2H,I), as observed for *Nrp1*-null mice (Gerhardt et al., 2004; Fantin et al., 2013a). Yet, the effect of the *Nrp1*<sup>Y297A/Y297A</sup> mutation on SVP angiogenesis was less severe than that of complete or endothelial-specific NRP1 loss, which causes a catastrophic failure of neighbouring vessels to interconnect, giving rise to large vascular tufts at vessel termini (Gerhardt et al., 2004; Fantin et al., 2013a). Importantly, the mild vascular defects in *Nrp1*<sup>Y297A/Y297A</sup> hindbrains do not phenocopy *Vegfa*<sup>120/120</sup> hindbrains expressing VEGF<sub>120</sub>, but lacking the NRP1-binding VEGF isoforms; specifically, *Vegfa*<sup>120/120</sup> hindbrains contain fewer pial vessels as well as poorly branched and enlarged vessels throughout the brain, and these defects can be attributed to perturbed VEGF gradients (Ruhrberg et al., 2002). As in the hindbrain, vessel density was only mildly affected in head and trunk of E9.5 *Nrp1*<sup>Y297A/Y297A</sup> embryos, and the formation of the pharyngeal arch arteries and the intersomitic vessels appeared to be unaffected (supplementary material Fig. S3). The mild vascular phenotype of *Nrp1*<sup>Y297A/Y297A</sup> embryos compared with the severe phenotype of *Nrp1*-null and *Vegfa*<sup>120/120</sup> mice argues against a major role for VEGF<sub>164</sub>-signalling through NRP1 in embryonic angiogenesis.

### Retinal angiogenesis and arteriogenesis are defective in *Nrp1*<sup>Y297A/Y297A</sup> mice

The impact of the Y297A mutation on postnatal vascular development was further investigated in the retina, where angiogenesis begins at P0 and is essentially complete by P21 (Fruttiger, 2007). Examination of the P7 retinal vasculature by wholemount immunofluorescence for the vascular marker collagen IV revealed a significant reduction in the extension of the primary vascular plexus towards the retinal margin in *Nrp1*<sup>Y297A/Y297A</sup> compared with WT retinas (Fig. 3A,B). The number of arteries and veins was also reduced in *Nrp1*<sup>Y297A/Y297A</sup> retinas (Fig. 3A,C; data not shown), and mutants displayed significantly reduced vessel coverage by vascular smooth muscle cells (VSMCs) positive for smooth muscle  $\alpha$ -actin (SMA) (Fig. 3A,D,E). Similar to the hindbrain, the *Nrp1*<sup>Y297A</sup> mutation greatly reduced NRP1 expression in *Nrp1*<sup>Y297A/Y297A</sup> compared with WT retinas (Fig. 3F).

By P21, delayed angiogenesis in the primary vascular plexus had largely recovered in homozygous mutants (Fig. 3G), but delayed formation of the deep and intermediate plexi was indicated by reduced vascular density (supplementary material Fig. S4). The number of arteries and their VSMC coverage remained significantly reduced (Fig. 3G-J). Moreover, incomplete vascularisation was observed in parts of the peripheral retinas, where vessels terminated in endothelial tufts covered with SMA-positive VSMCs and NG2 (CSPG4 – Mouse Genome Informatics)-positive pericytes (Fig. 3K). As NRP1 is not essential for endothelial cell proliferation (Jones et al., 2008), but is important for migration (Wang et al., 2003; Pan et al., 2007; Evans et al., 2011), tuft formation is likely to be due to abnormal endothelial cell sprouting. *Nrp1*<sup>Y297A/Y297A</sup> retinas also contained an increased number of arteriovenous crossings (Fig. 3L,M), similar to mice lacking the NRP1 cytoplasmic domain



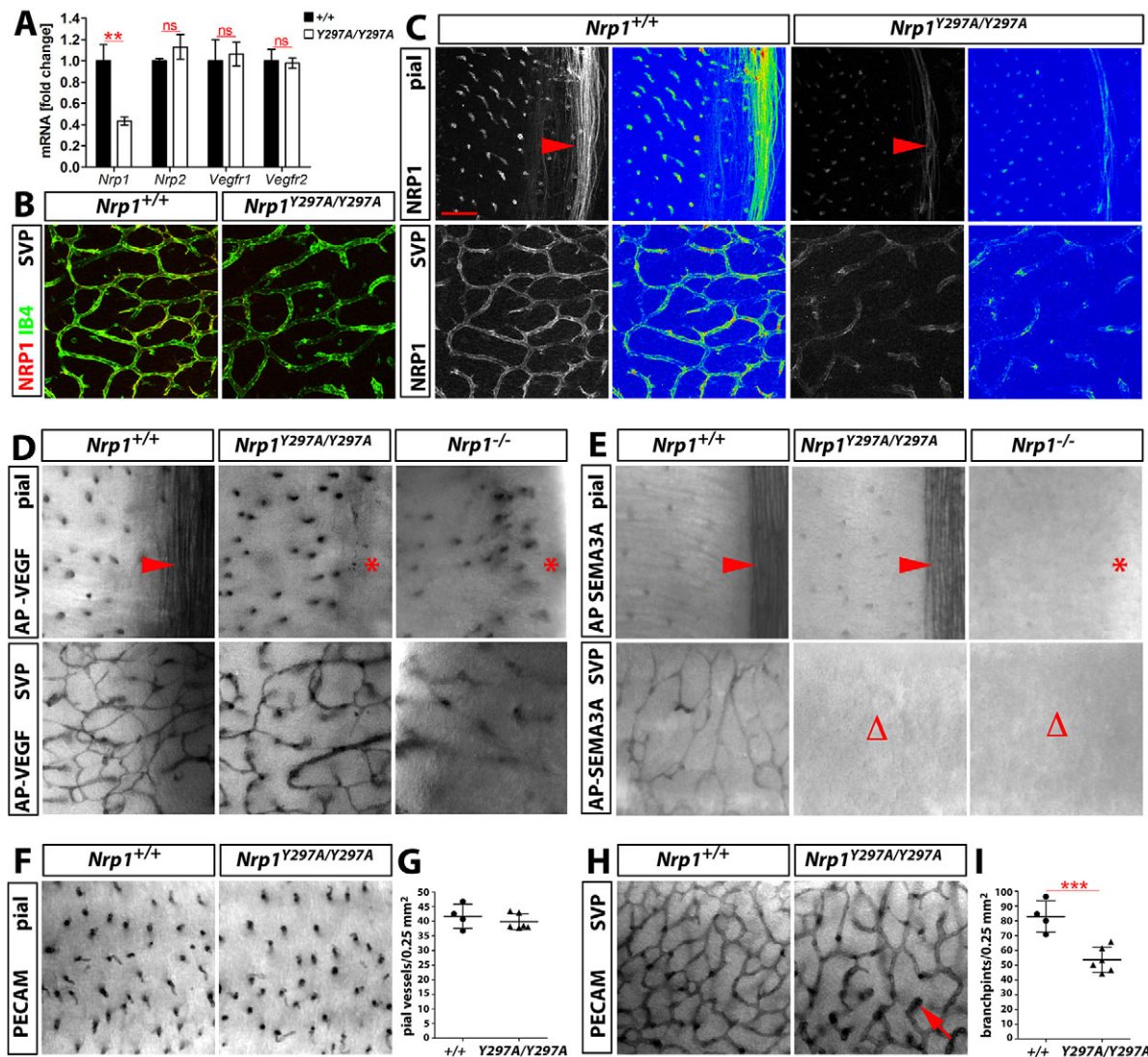


**Fig. 2. Mild angiogenesis defects in *Nrp1*<sup>Y297A/Y297A</sup> hindbrains.** (A–C) VEGF receptor expression in *Nrp1*<sup>Y297A/Y297A</sup> hindbrains. qPCR analysis for *Nrp1*, *Nrp2*, *Vegfr1* and *Vegfr2* relative to *Actb* (A) ( $n=3$ ; mean  $\pm$  s.d.; \*\* $P<0.01$ , ns, not significant) and whole-mount immunofluorescence staining for NRP1 and IB4 (B) in E11.5 hindbrains. (C) Single NRP1 channels are shown in greyscale and heat-map, blue and green indicate high, low and medium pixel intensity, respectively). Arrowheads indicate axons. (D,E) AP-VEGF<sub>165</sub> (D) and AP-SEMA3A (E) binding in E12.5 *Nrp1*<sup>Y297A/Y297A</sup> hindbrains; arrowheads indicate axons; asterisks highlight absent ligand binding to axons; open triangles indicate absent SEMA3A vessel binding. (F–I) Whole-mount PECAM immunostaining and quantification of vessels in E12.5 hindbrains, imaged (F) and quantified (G) on the pial side or imaged (H) and quantified (I) on the SVP side; the arrow indicates a vascular tuft;  $n\geq 4$ ; mean  $\pm$  s.d.; \*\*\* $P<0.001$ . Scale bar: in C, 100  $\mu$ m (B–F,H).

(Fantin et al., 2011) or with haploinsufficient expression of VEGF in the neural lineage (Haigh et al., 2003).

We cannot presently resolve whether low NRP1 expression levels and/or inhibition of VEGF<sub>165</sub> binding to NRP1 are primarily responsible for the observed retinal vascular defects in *Nrp1*<sup>Y297A/Y297A</sup> mice. However, their similarity to defects in *Vegfa*<sup>120/120</sup> retinas (Stalmans et al., 2002), combined with similar vascular defects in the P7 myocardium (Fig. 1M–P), suggests that NRP1-mediated VEGF-signalling is more important for perinatal than embryonic vascular development.

#### Reduced angiogenesis in *Nrp1*<sup>Y297A/Y297A</sup> mice with oxygen-induced retinopathy

The postnatal viability of *Nrp1*<sup>Y297A/Y297A</sup> mice allowed us to examine the impact of *Nrp1* hypomorphism and defective VEGF binding on pathological angiogenesis. We used a model of oxygen-induced

retinopathy, in which sequential exposure of neonatal mice to hyperoxia and normoxia causes obliteration of central retinal capillaries, followed by hypoxia-induced VEGF upregulation and abnormal neovascularisation (Smith et al., 1994). Vaso-obliteration was slightly reduced, consistent with reduced vascular dropout after hyperoxia or increased revascularisation of avascular areas after return to normoxia, whereas pathological neovascularisation was strongly and significantly decreased in *Nrp1*<sup>Y297A/Y297A</sup> compared with WT littermates (Fig. 4A–D). These observations show that NRP1 contributes substantially to ocular neovascularisation.

#### Reduced VEGF-induced angiogenesis and tumourigenesis in *Nrp1*<sup>Y297A/Y297A</sup> mice

VEGF stimulation of pathological angiogenesis in *Nrp1*<sup>Y297A/Y297A</sup> mice was assessed in the aortic ring assay, in which adult aortic explants undergo angiogenic sprouting upon growth factor

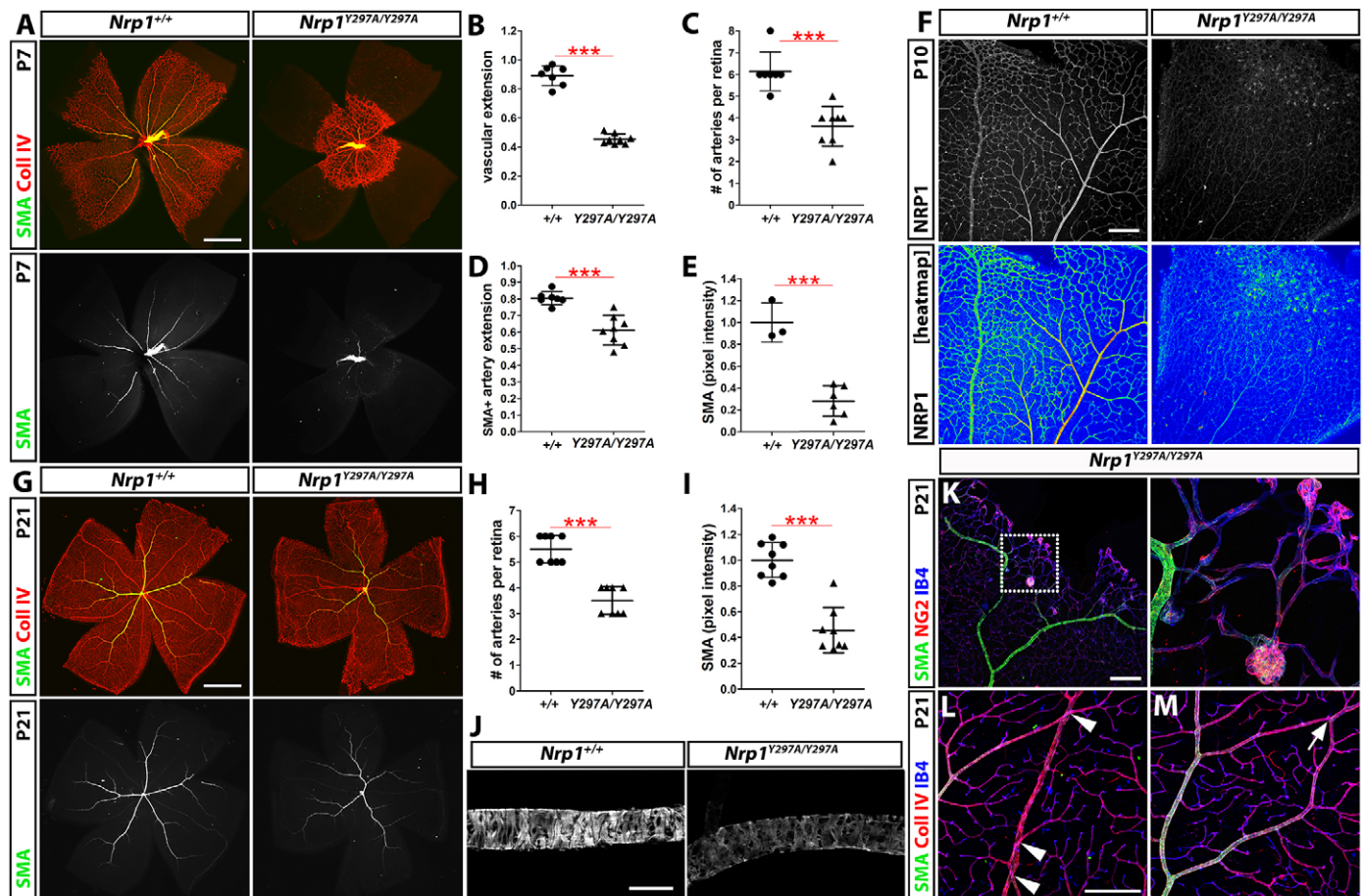


**Fig. 3. Defective retinal angiogenesis in *Nrp1*<sup>Y297A/Y297A</sup> mice.** (A–M) Immunostaining of retinal flatmounts and quantification of vascular patterning at P7 (A–E), P10 (F) and P21 (G–M). WT and *Nrp1*<sup>Y297A/Y297A</sup> littermates were immunolabelled for collagen IV and SMA (A, G, J; single SMA channel in greyscale), NRP1 (F; single NRP1 channel in greyscale and as pixel intensity heat-map) or IB4 and SMA with NG2 (K) or collagen IV (L, M). NRP1-positive cells at the mutant vascular front in F resemble macrophages normally observed at earlier stages of vascular development and therefore indicate delayed vascularisation. The area indicated with a dotted square in K is shown in higher magnification on the right. (L, M) Examples of defective main vessel segregation in *Nrp1*<sup>Y297A/Y297A</sup> mutants: multiple artery/vein crossings (L) and arterial anastomosis (M). Quantification of vascular extension (B), artery number (C, H), extension of SMA+ arteries (D) and arterial coverage by SMA+ VSMC (E, I);  $n \geq 3$ ; mean  $\pm$  s.d.; \*\*\* $P < 0.001$ . Scale bars: 1 mm (A, G); 200  $\mu$ m (F, K–M); 25  $\mu$ m (J).

stimulation (Baker et al., 2011). VEGF<sub>164</sub> increased vessel sprouting from WT aortic rings, but this response was suppressed by the *Nrp1*<sup>Y297A</sup> mutation (Fig. 4E–H). By contrast, serum stimulated sprouting from WT and mutant aortic rings similarly (Fig. 4H). We next examined the effect of the Y297A mutation on angiogenesis-dependent growth of syngeneic B16-F1 murine melanomas (Franco et al., 2002). These tumours produce high levels of VEGF, and their growth is blocked by VEGFR2 inhibition, demonstrating dependence on VEGF-driven angiogenesis (Prewett et al., 1999). Whereas tumours in WT mice grew rapidly, tumours were significantly smaller in age- and sex-matched *Nrp1*<sup>+/+/Y297A</sup> littermates and essentially absent in homozygotes at two weeks (>90% inhibition in homozygous mutants; Fig. 4I–L). Collectively, these genetic data show that NRP1 plays an important role in pathological angiogenesis driven by VEGF. Pan et al. (Pan et al., 2007) demonstrated that function-blocking antibodies targeting VEGF binding to NRP1 reduce human non-small cell lung carcinoma xenograft tumour size in mice by 37%. The greater effect of the Y297A mutation compared with blocking antibodies (>90% versus 37%) may reflect use of different tumour models and/or an additional effect of reducing NRP1 levels compared with inhibiting only VEGF binding to

NRP1, perhaps due to the contribution of ligands other than VEGF to tumour angiogenesis.

### Conclusions

The consensus model for the endothelial role of NRP1 is that it functions as a receptor for VEGF<sub>165</sub> and complexes with VEGFR2 to generate a holoreceptor that optimally transduces angiogenic signals. However, this model has hitherto been based almost entirely on biochemical and cell culture studies, combined with the analysis of a mouse model that abolishes all endothelial NRP1 functions. The severe reduction in NRP1 expression caused by the *Nrp1*<sup>Y297A</sup> allele did not permit definitive distinction of VEGF binding from other NRP1 functions requiring normal expression. However, the mild embryonic vascular phenotypes combined with the extended viability of *Nrp1*<sup>Y297A/Y297A</sup> relative to full and endothelial-specific NRP1 knockout mice clearly demonstrates for the first time that VEGF binding to NRP1 is not essential for embryonic angiogenesis and, therefore, that NRP1 functions in embryonic ECs predominantly in a VEGF-independent role. Because embryonic vascular functions of NRP1 do not involve semaphorin binding (Gu et al., 2003; Vieira et al., 2007), future studies will be needed to define the precise mechanism of NRP1 function in angiogenesis,



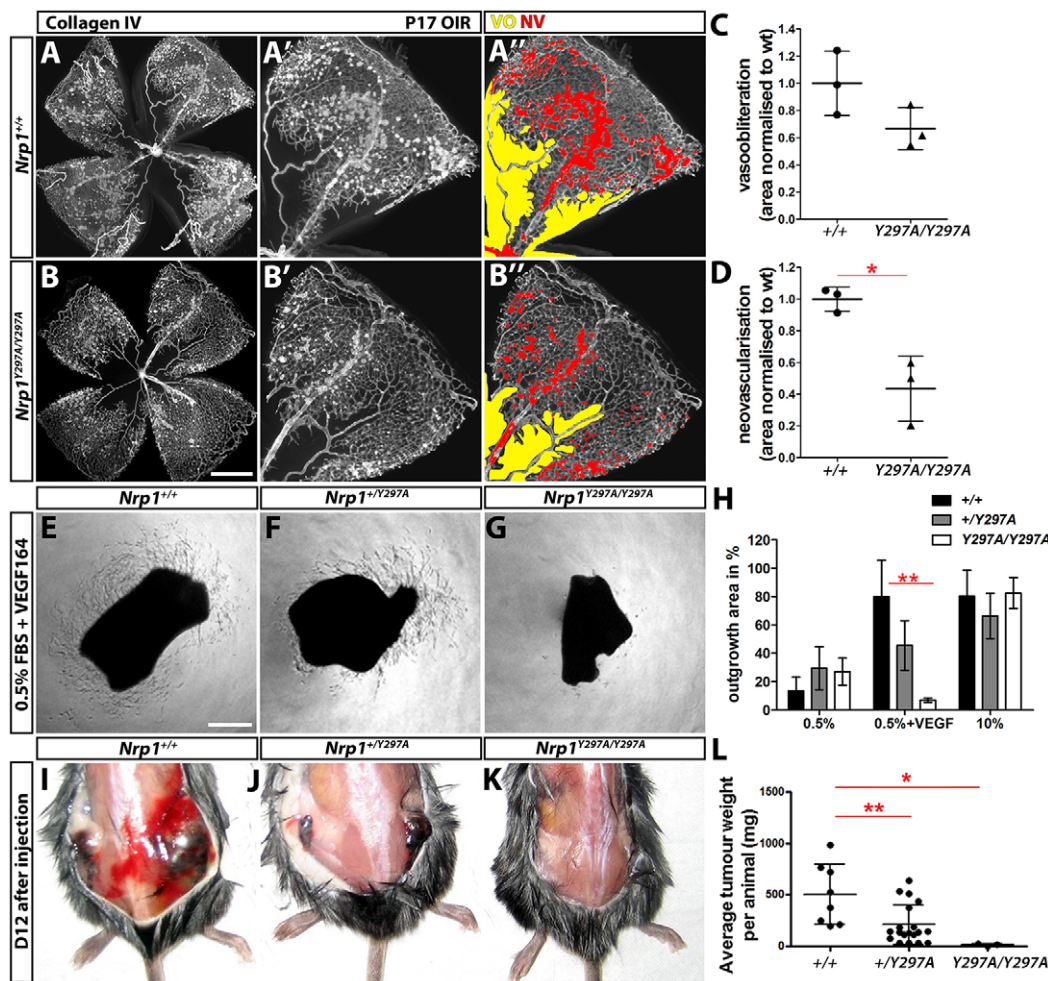


**Fig. 4. Reduced pathological angiogenesis and tumorigenesis in *Nrp1*<sup>Y297A/Y297A</sup> mice.** (A–D) Reduced angiogenesis in *Nrp1*<sup>Y297A/Y297A</sup> mice with oxygen-induced retinopathy. (A–B'') P17 retinal flatmounts from P17 *Nrp1*<sup>+/+</sup> (A–A'') and *Nrp1*<sup>Y297A/Y297A</sup> (B–B'') littermates were immunolabelled for collagen IV. Scale bar: 1 mm. Higher magnifications are shown in A', B', with pseudocoloured vaso-obliterated (VO, yellow) and neovascular (NV, red) areas in A'', B''. (C, D) Quantification of vaso-obliteration (C) and neovascularisation (D) in mutants relative to WT littermates. (E–H) Reduced VEGF-induced vessel sprouting in *Nrp1*<sup>Y297A/Y297A</sup> aortic rings. Aortic rings from adult WT (E), *Nrp1*<sup>+/Y297A</sup> (F) and *Nrp1*<sup>Y297A/Y297A</sup> (G) littermates were treated with 0.5% FBS ± 50 ng/ml VEGF<sub>164</sub> (E–G) or 10% FBS and the total area (H) of angiogenic sprouts quantified after 6 days;  $n \geq 4$ ; mean ± s.e.m. Scale bar: 250  $\mu$ m. (I–L) Reduced B16-F1 melanoma growth in *Nrp1*<sup>+/Y297A</sup> and *Nrp1*<sup>Y297A/Y297A</sup> mice. Representative tumours (I–K) and tumour weights (L) are shown;  $n \geq 3$ ; mean ± s.d.; \* $P < 0.05$ , \*\* $P < 0.01$ .

taking into account recent reports of NRP1 as a modulator of PDGF, TGF $\beta$  and integrin signalling (Valdembri et al., 2009; Cao et al., 2010; Evans et al., 2011; Pellet-Many et al., 2011; Yaqoob et al., 2012).

## MATERIALS AND METHODS

### Mice

Animal experiments were conducted in accordance with the Animal Care and Ethics Guidelines of University College London (UCL) and the United Kingdom Home Office Animals (Scientific Procedures) Act of 1986. Site-directed mutagenesis of mouse Y297 was performed as described (Herzog et al., 2011). The start codon and coding region of exon 2 of murine WT *Nrp1* were replaced by homologous recombination in 129Sv/Pas embryonic stem cells (ESCs) with murine cDNA containing *Nrp1*<sup>Y297A</sup>, targeted ESCs were injected into C57/BL6 blastocysts and resulting male F1 chimeras were bred with C57BL/6 females expressing CRE to generate heterozygous *Nrp1*<sup>+/Y297A</sup> mice lacking a neo cassette (Genoway; Lyon, France; Fig. 1). Genotyping and sequencing of genomic or cDNA from tail biopsies were performed with the primers listed in supplementary material Table S1.

### Expression studies

mRNA levels were measured by qPCR using cyclophilin as a normaliser and quantified with qStandard software (UCL). Protein expression in tissue lysates was determined by immunoblotting using rabbit anti-NRP1 (1:500; stock code 3725, Cell Signaling) and horseradish peroxidase-conjugated secondary antibody (1:10,000; stock code sc-2030, Santa Cruz), or immunostaining with goat anti-NRP1 (1:50; stock code AF566, R&D Systems) and biotinylated secondary antibody (1:200; stock code E0466, Dako).

### Assays

Cell culture, VEGF-binding assay, wholemount immunofluorescence, alkaline phosphatase (AP)-fusion protein binding assay, oxygen-induced retinopathy, aortic ring assays and tumour cell injections were all performed and quantified according to published procedures (Franco et al., 2002; Jia et al., 2006; Connor et al., 2009; Herzog et al., 2011; Baker et al., 2011; Fantin et al., 2013b).

### Statistics

Results are presented as means ± s.d. or s.e.m., as specified in each figure legend. Statistical significance of differences between samples was determined by a two-tailed Student's *t*-test; more than two datasets or grouped datasets were compared, respectively, by one-way or two-way analysis of variance followed by post-hoc tests. Genotype distribution was analysed using the  $\chi^2$  test, survival ratios using the Log-rank (Mantel-Cox) test. Statistical analyses were performed with Prism 5 (GraphPad Software);  $P < 0.05$  was considered significant.

### Acknowledgements

We thank the staff of the Biological Resources Units at the UCL Institute of Ophthalmology and the Wolfson Institute for Biomedical Research for help with mouse husbandry. We are grateful to the Imaging Facility at the UCL Institute of Ophthalmology for maintenance of the confocal microscopes.

### Competing interests

This study was financially assisted in part by Ark Therapeutics Ltd, which has had an interest in developing therapies to inhibit NRP1.

### Author contributions

A.F., B.H., C.R. and I.Z. designed the research, performed the research, analysed the data and wrote the paper. L.D. performed research. A.P., M.M. and M.Y. performed research and analysed the data.

## Funding

This work was supported by a British Heart Foundation (BHF) programme grant [RG/06/003 to I.Z., M.M. and M.Y.]; a BHF project grant [PG/10/86/28622 to C.R. and A.F.]; a BHF PhD studentship [FS/10/54/28680 to A.P.]; a Wellcome Trust New Investigator Award [095623/2/11/2 to C.R., A.F. and L.D.]; and Ark Therapeutics Ltd (B.H.). Deposited in PMC for immediate release.

## Supplementary material

Supplementary material available online at  
http://dev.biologists.org/lookup/suppl/doi:10.1242/dev.103028/-/DC1

## References

- Baker, M., Robinson, S. D., Lechertier, T., Barber, P. R., Tavora, B., D'Amico, G., Jones, D. T., Vojnovic, B. and Hodivala-Dilke, K. (2011). Use of the mouse aortic ring assay to study angiogenesis. *Nat. Protoc.* **7**, 89-104.
- Cao, Y., Szabolcs, A., Dutta, S. K., Yaqoob, U., Jagavelu, K., Wang, L., Leof, E. B., Urrutia, R. A., Shah, V. H. and Mukhopadhyay, D. (2010). Neuropilin-1 mediates divergent R-Smad signaling and the myofibroblast phenotype. *J. Biol. Chem.* **285**, 31840-31848.
- Carmeliet, P., Ng, Y. S., Nuyens, D., Theilmeier, G., Brusselmans, K., Cornelissen, I., Ehler, E., Kakkar, V. V., Stalmans, I., Mattot, V. et al. (1999). Impaired myocardial angiogenesis and ischemic cardiomyopathy in mice lacking the vascular endothelial growth factor isoforms VEGF164 and VEGF188. *Nat. Med.* **5**, 495-502.
- Connor, K. M., Krah, N. M., Dennison, R. J., Aderman, C. M., Chen, J., Guerin, K. I., Sapieha, P., Stahl, A., Willett, K. L. and Smith, L. E. (2009). Quantification of oxygen-induced retinopathy in the mouse: a model of vessel loss, vessel regrowth and pathological angiogenesis. *Nat. Protoc.* **4**, 1565-1573.
- Evans, I. M., Yamaji, M., Britton, G., Pellet-Many, C., Lockie, C., Zachary, I. C. and Frankel, P. (2011). Neuropilin-1 signaling through p130Cas tyrosine phosphorylation is essential for growth factor-dependent migration of glioma and endothelial cells. *Mol. Cell. Biol.* **31**, 1174-1185.
- Fantin, A., Vieira, J. M., Gestri, G., Denti, L., Schwarz, Q., Prykhodzhiy, S., Peri, F., Wilson, S. W. and Ruhrberg, C. (2010). Tissue macrophages act as cellular chaperones for vascular anastomosis downstream of VEGF-mediated endothelial tip cell induction. *Blood* **116**, 829-840.
- Fantin, A., Schwarz, Q., Davidson, K., Normando, E. M., Denti, L. and Ruhrberg, C. (2011). The cytoplasmic domain of neuropilin 1 is dispensable for angiogenesis, but promotes the spatial separation of retinal arteries and veins. *Development* **138**, 4185-4191.
- Fantin, A., Vieira, J. M., Plein, A., Denti, L., Fruttiger, M., Pollard, J. W. and Ruhrberg, C. (2013a). NRP1 acts cell autonomously in endothelium to promote tip cell function during sprouting angiogenesis. *Blood* **121**, 2352-2362.
- Fantin, A., Vieira, J. M., Plein, A., Maden, C. H. and Ruhrberg, C. (2013b). The embryonic mouse hindbrain as a qualitative and quantitative model for studying the molecular and cellular mechanisms of angiogenesis. *Nat. Protoc.* **8**, 418-429.
- Franco, S., Segura, I., Riese, H. H. and Blasco, M. A. (2002). Decreased B16F10 melanoma growth and impaired vascularization in telomerase-deficient mice with critically short telomeres. *Cancer Res.* **62**, 552-559.
- Fruttiger, M. (2007). Development of the retinal vasculature. *Angiogenesis* **10**, 77-88.
- Gerhardt, H., Ruhrberg, C., Abramsson, A., Fujisawa, H., Shima, D. and Betsholtz, C. (2004). Neuropilin-1 is required for endothelial tip cell guidance in the developing central nervous system. *Dev. Dyn.* **231**, 503-509.
- Gu, C., Limberg, B. J., Whitaker, G. B., Perman, B., Leahy, D. J., Rosenbaum, J. S., Ginty, D. D. and Kolodkin, A. L. (2002). Characterization of neuropilin-1 structural features that confer binding to semaphorin 3A and vascular endothelial growth factor 165. *J. Biol. Chem.* **277**, 18069-18076.
- Gu, C., Rodriguez, E. R., Reimert, D. V., Shu, T., Fritzsche, B., Richards, L. J., Kolodkin, A. L. and Ginty, D. D. (2003). Neuropilin-1 conveys semaphorin and VEGF signaling during neural and cardiovascular development. *Dev. Cell* **5**, 45-57.
- Haigh, J. J., Morelli, P. I., Gerhardt, H., Haigh, K., Tsien, J., Damert, A., Miquelot, L., Muhner, U., Klein, R., Ferrara, N. et al. (2003). Cortical and retinal defects caused by dosage-dependent reductions in VEGF-A paracrine signaling. *Dev. Biol.* **262**, 225-241.
- Herzog, B., Pellet-Many, C., Britton, G., Hatzoulakis, B. and Zachary, I. C. (2011). VEGF binding to NRP1 is essential for VEGF stimulation of endothelial cell migration, complex formation between NRP1 and VEGFR2, and signaling via FAK Tyr407 phosphorylation. *Mol. Biol. Cell* **22**, 2766-2776.
- Jarvis, A., Allerton, C. K., Jia, H., Herzog, B., Garza-Garcia, A., Winfield, N., Ellard, K., Aqil, R., Lynch, R., Chapman, C. et al. (2010). Small molecule inhibitors of the neuropilin-1 vascular endothelial growth factor A (VEGF-A) interaction. *J. Med. Chem.* **53**, 2215-2226.
- Jia, H., Bagherzadeh, A., Hatzoulakis, B., Jarvis, A., Löhr, M., Shaikh, S., Aqil, R., Cheng, L., Tickner, M., Esposito, D. et al. (2006). Characterization of a bicyclic peptide neuropilin-1 (NP-1) antagonist (EG3287) reveals importance of vascular endothelial growth factor exon 8 for NP-1 binding and role of NP-1 in KDR signaling. *J. Biol. Chem.* **281**, 13493-13502.
- Jones, E. A., Yuan, L., Breant, C., Watts, R. J. and Eichmann, A. (2008). Separating genetic and hemodynamic defects in neuropilin 1 knockout embryos. *Development* **135**, 2479-2488.
- Kawasaki, T., Kitsukawa, T., Bekku, Y., Matsuda, Y., Sanbo, M., Yagi, T. and Fujisawa, H. (1999). A requirement for neuropilin-1 in embryonic vessel formation. *Development* **126**, 4895-4902.
- Kitsukawa, T., Shimizu, M., Sanbo, M., Hirata, T., Taniguchi, M., Bekku, Y., Yagi, T. and Fujisawa, H. (1997). Neuropilin-semaphorin III/D-mediated chemorepulsive signals play a crucial role in peripheral nerve projection in mice. *Neuron* **19**, 995-1005.
- Lanahan, A., Zhang, X., Fantin, A., Zhuang, Z., Rivera-Molina, F., Speichinger, K., Praht, C., Zhang, J., Wang, Y., Davis, G. et al. (2013). The neuropilin 1 cytoplasmic domain is required for VEGF-A-dependent arteriogenesis. *Dev. Cell* **25**, 156-168.
- Ng, Y. S., Rohan, R., Sunday, M. E., Demello, D. E. and D'Amore, P. A. (2001). Differential expression of VEGF isoforms in mouse during development and in the adult. *Dev. Dyn.* **220**, 112-121.
- Pan, Q., Chanthery, Y., Liang, W. C., Stawicki, S., Mak, J., Rathore, N., Tong, R. K., Kowalski, J., Yee, S. F., Pacheco, G. et al. (2007). Blocking neuropilin-1 function has an additive effect with anti-VEGF to inhibit tumor growth. *Cancer Cell* **11**, 53-67.
- Pellet-Many, C., Frankel, P., Jia, H. and Zachary, I. (2008). Neuropilins: structure, function and role in disease. *Biochem. J.* **411**, 211-226.
- Pellet-Many, C., Frankel, P., Evans, I. M., Herzog, B., Jünemann-Ramírez, M. and Zachary, I. C. (2011). Neuropilin-1 mediates PDGF stimulation of vascular smooth muscle cell migration and signalling via p130Cas. *Biochem. J.* **435**, 609-618.
- Prewett, M., Huber, J., Li, Y., Santiago, A., O'Connor, W., King, K., Overholser, J., Hooper, A., Pytowski, B., Witte, L. et al. (1999). Antivascular endothelial growth factor receptor (fetal liver kinase 1) monoclonal antibody inhibits tumor angiogenesis and growth of several mouse and human tumors. *Cancer Res.* **59**, 5209-5218.
- Raimondi, C. and Ruhrberg, C. (2013). Neuropilin signalling in vessels, neurons and tumours. *Semin. Cell Dev. Biol.* **24**, 172-178.
- Ruhrberg, C., Gerhardt, H., Golding, M., Watson, R., Ioannidou, S., Fujisawa, H., Betsholtz, C. and Shima, D. T. (2002). Spatially restricted patterning cues provided by heparin-binding VEGF-A control blood vessel branching morphogenesis. *Genes Dev.* **16**, 2684-2698.
- Smith, L. E., Wesolowski, E., McLellan, A., Kostyk, S. K., D'Amato, R., Sullivan, R. and D'Amore, P. A. (1994). Oxygen-induced retinopathy in the mouse. *Invest. Ophthalmol. Vis. Sci.* **35**, 101-111.
- Soker, S., Miao, H. Q., Nomi, M., Takashima, S. and Klagsbrun, M. (2002). VEGF165 mediates formation of complexes containing VEGFR-2 and neuropilin-1 that enhance VEGF165-receptor binding. *J. Cell. Biochem.* **85**, 357-368.
- Stalmans, I., Ng, Y. S., Rohan, R., Fruttiger, M., Bouché, A., Yuce, A., Fujisawa, H., Hermans, B., Shani, M., Jansen, S. et al. (2002). Arteriolar and venular patterning in retinas of mice selectively expressing VEGF isoforms. *J. Clin. Invest.* **109**, 327-336.
- Tomanek, R. J. (1996). Formation of the coronary vasculature: a brief review. *Cardiovasc. Res.* **31**, E46-E51.
- Valdembri, D., Caswell, P. T., Anderson, K. I., Schwarz, J. P., König, I., Astanina, E., Caccavari, F., Norman, J. C., Humphries, M. J., Bussolino, F. et al. (2009). Neuropilin-1/GIPC1 signaling regulates alpha5beta1 integrin traffic and function in endothelial cells. *PLoS Biol.* **7**, e25.
- Vander Kooi, C. W., Jusino, M. A., Perman, B., Neau, D. B., Bellamy, H. D. and Leahy, D. J. (2007). Structural basis for ligand and heparin binding to neuropilin B domains. *Proc. Natl. Acad. Sci. USA* **104**, 6152-6157.
- Vieira, J. M., Schwarz, Q. and Ruhrberg, C. (2007). Selective requirements for NRP1 ligands during neurovascular patterning. *Development* **134**, 1833-1843.
- von Wronski, M. A., Raju, N., Pillai, R., Bogdan, N. J., Marinelli, E. R., Nanjappan, P., Ramalingam, K., Arunachalam, T., Eaton, S., Linder, K. E. et al. (2006). TGF-beta binds neuropilin-1 through a sequence similar to that encoded by exon 8 of vascular endothelial growth factor. *J. Biol. Chem.* **281**, 5702-5710.
- Wang, L., Zeng, H., Wang, P., Soker, S. and Mukhopadhyay, D. (2003). Neuropilin-1-mediated vascular permeability factor/vascular endothelial growth factor-dependent endothelial cell migration. *J. Biol. Chem.* **278**, 48848-48860.
- Yaqoob, U., Cao, S., Shergill, U., Jagavelu, K., Geng, Z., Yin, M., de Assuncao, T. M., Cao, Y., Szabolcs, A., Thorgeirsson, S. et al. (2012). Neuropilin-1 stimulates tumor growth by increasing fibronectin fibril assembly in the tumor microenvironment. *Cancer Res.* **72**, 4047-4059.